

**NORTHWESTERN UNIVERSITY**  
**McCORMICK SCHOOL OF ENGINEERING**  
**AND APPLIED SCIENCE**

DEPARTMENT OF MATERIALS SCIENCE  
AND ENGINEERING

TECHNICAL REPORT #34

OFFICE OF NAVAL RESEARCH

MAY 1997

CONTRACT NO. N00014-80-C-116

---

---

X-Ray Diffraction and Finite Element Study of Residual Stress Effects on Fatigue Crack Growth

by

J. D. Almer, J. B. Cohen, K. R. McCallum, and R. A. Winholtz

---

---

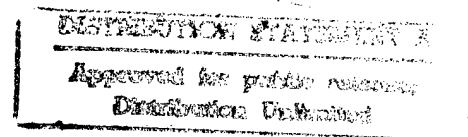
Distribution of this document is unlimited

Reproduction in whole or in part is permitted for any  
purpose of the United States Government



EVANSTON, ILLINOIS

DTIC QUALITY INSPECTED 2



19970616 107

## X-Ray Diffraction and Finite Element Study of Residual Stress Effects on Fatigue Crack Growth

J.D. Almer<sup>†</sup>, J.B. Cohen<sup>†</sup>, K.R. McCallum\* and R.A. Winholtz\*

<sup>†</sup> McCormick School of Engineering and Applied Science, Northwestern University,  
Evanston, IL, 60201, USA

\* Mechanical and Aerospace Engineering Department, University of Missouri, Columbia,  
MO 65211, USA

### ABSTRACT

The combined techniques of microbeam x-ray diffraction and Finite Element (FE) analysis have been used to analyze the residual stresses resulting from an interference operation in 1080 steel. Both techniques showed the resulting stresses to be tensile, and accelerated growth rates were observed in fatigue cracks subsequently grown into this residual stress field. The growth rates also showed a clear sensitivity to applied stress intensity level. Through-thickness residual stress variations as predicted by FE analysis help explain observed crack front shapes.

### INTRODUCTION

Whether formed during processing operations or accrued in service, materials will often contain residual stresses. In structures undergoing fatigue loading these residual stresses can alter actual loading conditions and affect the growth of fatigue cracks. Thus there have been a number of studies undertaken to examine residual stress effects on fatigue crack growth (see [1] for a review). Although compressive residual stresses have been almost universally found to decrease growth rates, the effect of tensile residual stresses is not as clear. Although some evidence for accelerated growth rates in the presence of tensile stresses exists [2] several materials, including steels, have shown these stresses to have little or no effect on stage II crack growth. The lack of mean (tensile) stress sensitivity in the Paris growth regime has been linked to stress fading near the crack tip, which will vary depending on the applied stress intensity level [3].

Comprehensive analysis of residual stress effects requires stress information throughout the body of the a material, which may be obtained by including through-thickness Finite Element (FE) stress analysis along with surface sensitive x-ray diffraction measurements. With the advent of greater speed and flexibility in computer systems FE modeling of quantities such as residual stresses and plastic deformation is taking on an increased role in structural analysis. Confident use of FE to model real problems, however, necessitates comparison with experimental results and a dearth of such studies exists. Therefore a FE code was used to model the development of tensile residual stresses from an interference operation and meshed to compare directly near-surface residual stresses with measured x-ray values. Reasonable agreement was obtained, and FE predictions of through-thickness residual stress variations helped explain observed crack front shapes.

### EXPERIMENTAL PROCEDURE

#### Specimens and FE Mesh

As received 1080 steel (12.4mm thickness) was heat treated to produce a fine grained, spheroidized microstructure. The resulting average ferrite grain size and cementite particle size was 5 and 0.7 $\mu$ m, respectively, with a 13.1(6)% cementite volume fraction as determined from x-ray powder diffraction. Both sides of the steel were electropolished

2

to remove 0.45mm from each face, resulting in smooth surfaces free of decarburized layers as verified by hardness measurements.

Compact-tension (CT) specimens were machined from the bulk steel as per ASTM standards [4], and residual stresses were introduced ahead of the future crack planes by drilling tapered holes and then expanding the holes by inserting case-hardened and tapered steel plugs at 0.95% radial interference strain (fig 1(a)). The tapering was necessary to allow uniform through-thickness pressure to be applied during the interference, but led to an ~8% larger stress on the bottom surface relative to the top due to differences in plug diameter. Through-thickness stress variations arising from frictional sliding across the plug/plate interface were also expected, underscoring the importance of through-thickness stress information provided by our FE model in addition to surface-sensitive x-ray measurements. 'Control' specimens were also produced without the hole and with the hole but without the plug for direct comparison of crack growth rates.

The interference-fit operation was modeled along the future (x-z) crack plane by FE as shown in fig.1(b). Due to the radial symmetry of the operation this x-z slice was modeled axisymmetrically, with the center of the plug serving as the axis of symmetry. The interference was simulated by forcing the plug to expand under eigenstrains corresponding to the applied interference:

$$\epsilon_x^* = \epsilon_y^* = \delta / (R_0 + mz) = 0.03302 / (3.5 + 0.0104z) \quad (1)$$

$$\epsilon_z^* = 0.003z \quad (2)$$

where  $\delta$  is the constant radial misfit,  $R_0$  is the radius of the top of the plug (at  $z=0$ ),  $m$  is the taper angle in radians and  $z$  is in mm. The  $z$ -dependence of the  $x$  and  $y$  eigenstrains accounts for the linear variation in strain (and stress) along  $z$  in accordance with experiment. The  $z$ -component of eigenstrain simulates the frictional force experienced by the plug/plate interface. Its value was determined empirically by matching the FE-simulated surface displacements with experimental values measured with a surface profilometer (not shown). The FE mesh was graded towards both surfaces and the interface - with the smallest surface elements  $5\mu\text{m}$  in height and approximately  $200\mu\text{m}$  in width near the interface. This allows for direct comparison with x-ray data taken with the  $200\mu\text{m}$  beam as the  $1/e$  penetration depth for Cr in Fe is approximately  $5\mu\text{m}$ . The resulting mesh was comprised of 3520 total elements. Material parameters for 1080 steel were determined from uniaxial stress/strain data ( $\sigma_y=550\text{MPa}$ ,  $E=215\text{GPa}$ ), and input into the Finite Element Analysis Package [5] for stress analysis. The steel showed no appreciable work hardening out to the maximum plastic strain ranges computed by FE and so was modeled as elastic-perfectly plastic, while the much harder plug was taken to be elastic throughout with the same modulus as the plug.

### Fatigue Testing

The CT specimens were notched with a jeweler's saw and pre-cracked by applying a high tensile load, which was then decreased in steps to grow the cracks into the stable stage II regime at the desired  $\Delta K$  values. These stage II fatigue cracks were cycled at  $R=0.1$  and constant  $\Delta K$  at levels ranging from  $19.5\text{--}25\text{MPa}\sqrt{\text{m}}$ . Through-thickness crack growth was monitored by measuring specimen compliance with a clip gage and periodically checked with an optical microscope until sample failure into the plug interface.

## X-ray Microbeam Stress Analysis

Diffraction methods are widely used for stress analysis due to their relatively non-destructive nature and ability to measure the entire stress tensor.[6] This analysis is based on measuring average lattice strains from diffraction peak shifts, which are converted to stresses using measured elastic constants. In multiphase materials the stresses can be measured in each phase allowing separation into macrostress and microstress components.

Here we used triaxial stress analysis to measure both in- and out-of-plane stress components via a least-squares procedure[7], and separated stresses into macro- and microstresses in each phase using the measured cementite volume fraction and equations of microstress equilibrium [8].

In order to measure stress gradients generated near the plug interface an x-ray microbeam of 210 $\mu\text{m}$  diameter was used. Since beam intensity is proportional to area such a microbeam is relatively weak - thus we designed our system to maximize flux and efficiency. A tapered glass capillary was developed to focus x-rays produced by a 12 kW rotating anode source with a Cr target. The capillary provides a threefold increase in intensity, and comparable increase in divergence, as compared to an equivalent pinhole collimator. The Fe 211 peaks were measured with a position sensitive detector while a solid-state detector was used for the weaker Fe<sub>3</sub>C 250 peaks in order to increase the peak/background ratio. Further details of the experimental setup and measurements are given in [9].

## RESULTS AND DISCUSSION

### X-ray and FE Residual Stresses from Interference Fit

Comparisons between the measured and simulated residual stresses formed in the near-surface regions ( $\leq 5\mu\text{m}$ ) of the plate are shown in fig2(a,c). The deviatoric stresses  $\sigma_{yy}$  are shown since these will most strongly affect the crack during mode I loading. Plastic deformation as evidenced from diffraction line broadening was measured out to 4mm from the interface. Within this plastic region the cementite takes up a higher fraction of the load than the ferrite, leading to microstresses in addition to a tensile macrostress. The FE method qualitatively reproduces these measured macrostresses on both surfaces of the plate, though it overestimates their magnitude near the interface.

By qualitatively matching the measured surface macrostresses FE predictions of  $\sigma_{yy}^M$  throughout the crack plane, fig.2(c), can be used with greater confidence to predict z-variations in residual stress and therefore crack front shape. Two major trends seen from the FE predictions are that the tensile stresses are greatest at the surfaces of the plate and that the frictional sliding simulated along the plug/plate interface has led to especially high tensile stresses near the top of the plate relative to the bottom portion. Thus as the crack approaches the interface growth is expected to be accelerated at the surface relative to the bulk, especially towards the top surface of the plate.

### Fatigue Crack Growth Rates and Crack Front Shape

Fatigue cracks grown into the tensile stress fields were significantly affected by these stresses as shown in fig 3(a). In this figure the propagation rates at each  $\Delta K$  were normalized by the rates of control samples grown at equal  $\Delta K$ , thus limiting any differences in growth rates to residual stress effects. The tensile residual stresses increase

crack growth rates by up to two orders of magnitude near the plug. Furthermore, the distance at which the crack begins accelerating shows a strong dependence on  $\Delta K$ . At  $\Delta K=19.5 \text{ MPa}\sqrt{\text{m}}$  the crack begins to accelerate at  $a/c=0.74$  (6.5mm from the plug/plate interface) while as  $\Delta K$  is increased the acceleration is progressively retarded to distances closer to the interface. This implies that the crack becomes more 'sensitive' to residual stresses at lower applied  $\Delta K$ . Once the acceleration has begun at a given  $\Delta K$ , however, it proceeds at a higher rate with increasing  $\Delta K$ , which may be associated with a transition from stage II to catastrophic stage III growth under the combination of high applied and residual tensile stresses. To ensure that these effects are not geometrically based we grew a crack into a sample containing a hole without the plug and found crack growth to be unaffected (insert). This shows that the residual stresses, rather than geometrical effects, are causing the observed acceleration.

Fractographic analysis on the sample grown at  $\Delta K=22.5 \text{ MPa}\sqrt{\text{m}}$  into the plug stress field, fig.3(b), illustrates the effect of the through-thickness stress variations as predicted by FE. While crack fronts in control samples showed bowing towards the interior due to the plane strain (high driving force) conditions relative to the plane stress conditions at the surface, the crack fronts in the plug sample are quite different. At 3mm from the interface (position A in the figure) the crack front is rather linear, evidence that the higher surface stresses (relative to the bulk) have accelerated surface growth, while closer to the plug (position B) the crack has grown asymmetrically towards the position of maximum  $\sigma_{yy}^M$  as predicted by FE (fig.2(b)).

## CONCLUSIONS

1. An interference fit in 1080 steel resulted in a complex residual stress field, primarily consisting of tensile macrostresses, which was characterized by microbeam x-ray diffraction and comparative Finite Element (FE) analysis.
2. These tensile stresses significantly accelerated fatigue crack growth rates, with increasing crack sensitivity to the residual stresses observed with decreasing applied stress intensity.
3. Through-thickness residual stress variations as predicted by FE analysis help explain observed crack front shapes and thus highlight the usefulness of FE in conjunction with comparative experimental analysis to understand residual stress effects in fatigue.

## ACKNOWLEDGMENTS

This research was funded by the Office of Naval Research under contract no. N00014-90-J-1374. We wish to thank Prof. B. Moran and L. Wittig-Cordes from the Civil Engineering department at NU for their assistance with the Finite Element analysis.

## REFERENCES

1. Parker, A.P., "Stress Intensity Factors, Crack Profiles, and Fatigue Crack Growth Rates in Residual Stress Fields", ASTM STP 776, 13 (1982).
2. Nelson, D.V., "Effects of Residual Stress on Fatigue Crack Propagation", ASTM STP 776, 172 (1982).
3. Saxena, A. and S.J. Hudak, "Role of Crack-Tip Stress Relaxation in Fatigue Crack Growth", ASTM STP 677 (1979).
4. ASTM, "Standard Test Method for Measurement of Fatigue Crack Growth Rates", Report # E 647-88a, (1989).

5. Zienkiewicz, O.C. and R.L. Taylor, *The Finite Element Method*. 4 ed, New York: McGraw Hill (1989).
6. Noyan, I.C. and J.B. Cohen. *Residual Stress: Measurement by Diffraction and Interpretation*, New York: Springer Verlag (1986).
7. Winholtz, R.A. and J.B. Cohen, "Generalized Least-Squares Determination of Triaxial Stress States by X-ray Diffraction and the Associated Errors", *Aust. J. Phys.*, **41**, 189 (1988).
8. Noyan, I.C., "Equilibrium Conditions for the Average Stresses Measured by X-Rays", *Met. Trans. A*, **14A**, 1907 (1983).
9. Almer, J.D., J.B. Cohen, W.D. Kirk, and R.A. Winholtz, in *Adv. in X-Ray Anal.*, Colorado Springs, CO: Plenum Press (1995).

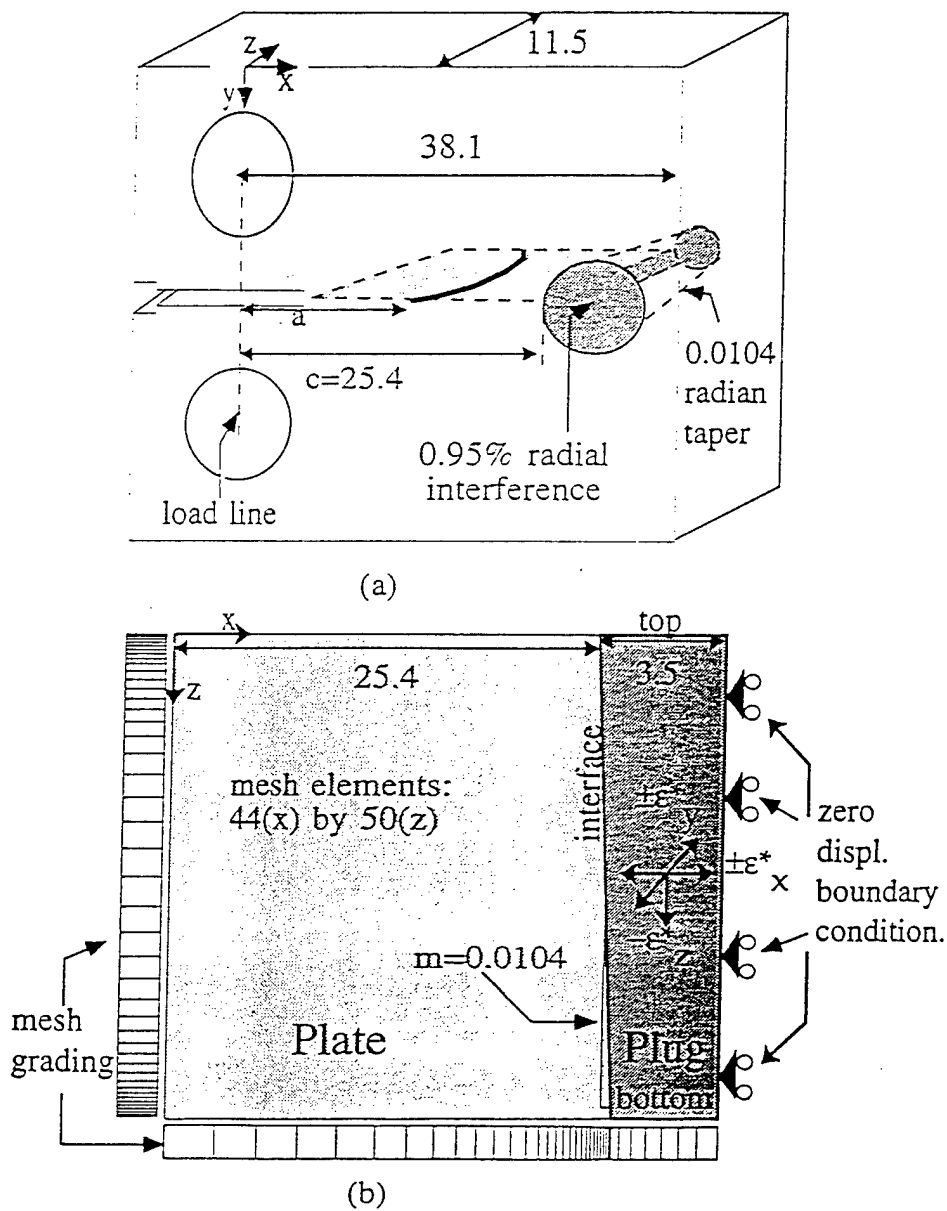


Figure 1: Geometry for (a) CT specimen and (b) corresponding Finite Element slice, with element grading and displacement boundary conditions shown on mesh edges. Unless given, all dimensions in mm.

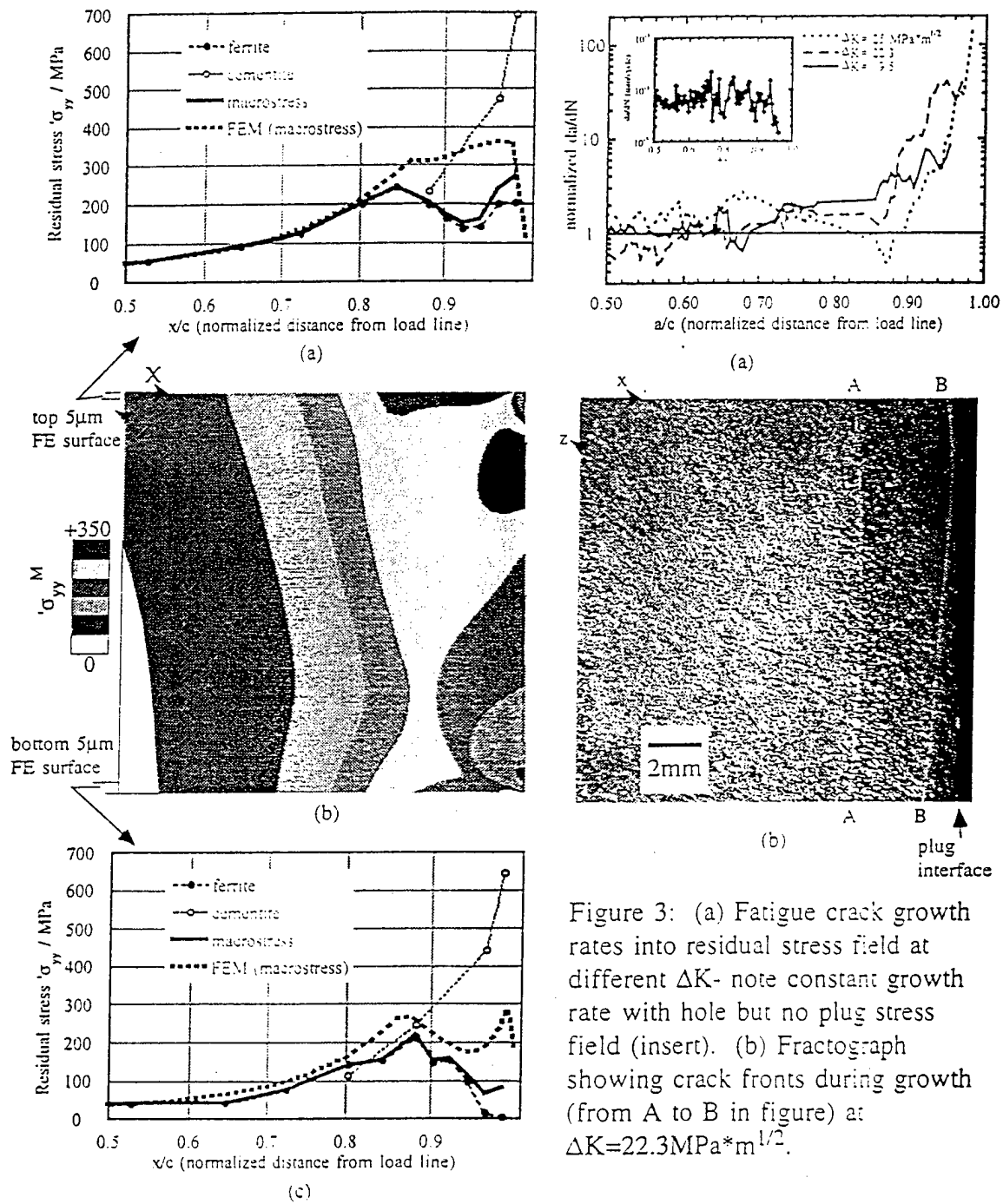


Figure 2: Deviatoric residual stresses  $\sigma_{yy}$  in 1080 plate resulting from the interference fit: (a,c) comparison of x-ray and FE simulated stresses in top and bottom 5µm surface layers and (b) through-thickness FE stresses. Plug interface is at  $x/c=1.0$ .

Figure 3: (a) Fatigue crack growth rates into residual stress field at different  $\Delta K$ - note constant growth rate with hole but no plug stress field (insert). (b) Fractograph showing crack fronts during growth (from A to B in figure) at  $\Delta K=22.3 \text{ MPa}\cdot\text{m}^{1/2}$ .

## DOCUMENT CONTROL DATA - R &amp; D

*(Security classification of title, body of abstract and indexing annotation must be entered when the overall report is classified)*

1. ORIGINATING ACTIVITY (Corporate author)

J. B. Cohen  
 McCormick School of Engineering  
 Northwestern University, Evanston, IL 60208

2a. REPORT SECURITY CLASSIFICATION

2b. GROUP

3. REPORT TITLE

X-Ray Diffraction and Finite Element Study of Residual Stress Effects on  
 Fatigue Crack Growth

4. DESCRIPTIVE NOTES (Type of report and inclusive dates)

Technical Report 34

5. AUTHOR(S) (First name, middle initial, last name)

J. D. Almer, J. B. Cohen, K. R. McCallum, and R. A. Winholtz

6. REPORT DATE

May 1997

7a. TOTAL NO. OF PAGES

7

7b. NO. OF REFS

8a. CONTRACT OR GRANT NO.

9a. ORIGINATOR'S REPORT NUMBER(S)

34

9b. OTHER REPORT NO(S) (Any other numbers that may be assigned this report)

b. PROJECT NO.

c.

d.

10. DISTRIBUTION STATEMENT

Distribution of document is unlimited

11. SUPPLEMENTARY NOTES

12. SPONSORING MILITARY ACTIVITY

Metallurgy Branch  
 Office of Naval Research

13. ABSTRACT

The combined techniques of microbeam x-ray diffraction and Finite Element (FE) analysis have been used to analyze the residual stresses resulting from an interference operation in 1080 steel. Both techniques showed the resulting stresses to be tensile, and accelerated growth rates were observed in fatigue cracks subsequently grown into this residual stress field. The growth rates also showed a clear sensitivity to applied stress intensity level. Through-thickness residual stress variations as predicted by FE analysis help explain observed crack front shapes.